JOC*Article*

Z/*E*-Photoisomerizations of Olefins with $4n\pi$- or $(4n + 2)\pi$-Electron Substituents: Zigzag Variations in Olefin Properties along the T_1 State Energy Surfaces

Haruhisa Kato,[†,||] Maria Brink,[‡] Helene Möllerstedt,[‡,⊥] Mari Carmen Piqueras,[§] Raül Crespo,[§] and Henrik Ottosson*[,†]

Department of Chemistry and Biomolecular Sciences, Chalmers University of Technology, 412 96 Göteborg, Sweden, Departament de Química Física, Universitat de València, Dr. Moliner 50, E-46100 Burjassot, Spain, and Department of Chemistry (Organic Chemistry), Uppsala University, Box 599, 751 24 Uppsala, Sweden

Henrik.Ottosson@kemi.uu.se

Received July 26, 2005

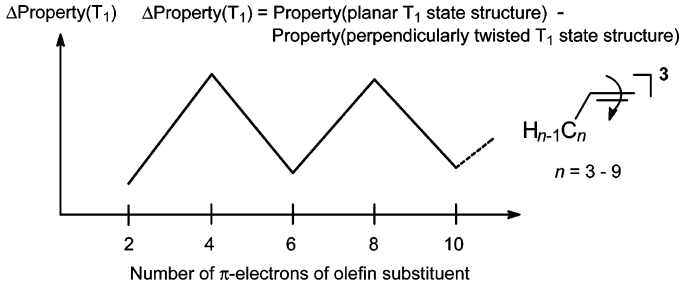

A quantum chemical study has been performed to assess changes in aromaticity along the T_1 state *Z*/*E*-isomerization pathways of annulenyl-substituted olefins. It is argued that the point on the T_1 energy surface with highest substituent aromaticity corresponds to the minimum. According to Baird (*J. Am. Chem. Soc*. **1972**, *94*, 4941), aromaticity and antiaromaticity are interchanged when going from S_0 to T_1. Thus, olefins with S_0 aromatic substituents (set **A** olefins) will be partially antiaromatic in T_1 and vice versa for olefins with S_0 antiaromatic substituents (set **B** olefins). Twist of the C=C bond to a structure with a perpendicular orientation of the 2p(C) orbitals (^{3}p*) in T_1 should lead to regaining substituent aromaticity in set **A** and loss of aromaticity in set **B** olefins. This hypothesis is verified through quantum chemical calculations of T_1 energies, geometries (bond lengths and harmonic oscillator measure of aromaticity), spin densities, and nucleus independent chemical shifts whose differences along the T_1 PES display zigzag dependencies on the number of π-electrons in the annulenyl substituent of the olefin. Aromaticity changes are reflected in the profiles of the T_1 potential energy surfaces (T_1 PESs) for *Z*/*E*-isomerizations because olefins in set **A** have minima at ^{3}p* whereas those in set **B** have maxima at such structures. The proper combination (fusion) of the substituents of set **A** and **B** olefins could allow for design of novel optical switch compounds that isomerize adiabatically with high isomerization quantum yields.

Introduction

In 1972, Baird used perturbation molecular orbital (PMO) theory to derive that annulenes that are aromatic in their singlet ground states (S_0) are antiaromatic in their lowest triplet excited states (T_1) and vice versa.[1] This theory was later examined by Schleyer and coworkers through quantum chemical B3LYP, CCSD(T), and GIAO-HF calculations of a series of $4n\pi$-electron annulenes that are antiaromatic in S_0.[2] Aromatic stabilization energies, CC bond lengths, and nucleus independent chemical shifts (NICS)[3] were used to confirm the aromaticity of $4n\pi$-annulenes in T_1. The high level

[†] Uppsala University.
[‡] Chalmers University of Technology.
[§] Universitat de València.
[||] Present address: National Metrology Institute of Japan (NMIJ), National Institute of Advanced Industrial Science and Technology (AIST) Tsukuba Central 5, Higashi 1-1-1, Tsukuba, Ibaraki, 305-8565 Japan.
[⊥] Present address: Canea AB, Packhusgatan 6, SE-411 13 Gothenburg, Sweden.

(1) Baird, N. C. *J. Am. Chem. Soc.* **1972**, *94*, 4941.
(2) Gogonea, V.; Schleyer, P. v. R.; Schreiner, P. R. *Angew. Chem., Int. Ed.* **1998**, *37*, 1945.
(3) Schleyer, P. v. R.; Maerker, C.; Dransfeld, A.; Jiao, H.; Hommes, N. J. R. v. E. *J. Am. Chem. Soc.* **1996**, *118*, 6317.

10.1021/jo051558y CCC: $30.25
Published on Web 10/08/2005

computations[2] thus verified Baird's theory,[1] which is important for interpretation of processes that take place in T_1.

In photochemistry, *Z*/*E*-photoisomerization of olefins holds a central position,[4] and it is one of the key photochemical processes utilized in functional materials as well as in molecular switch and motor design.[5,6] For example, sterically overcrowded alkenes that photoisomerize constitute the core of the chiroptical molecular switches and unidirectional molecular rotary motors of Feringa and co-workers.[7] Recently, the *Z*/*E*-photoisomerization of alkenes and azobenzenes has also been exploited in molecular electronics to optically switch electron transport[8,9] and to photomechanically control the electronic properties of linear π-conjugated systems.[10]

Z/*E*-Photoisomerization occurs in both singlet and triplet excited states; however, herein we focus on isomerizations that occur in the triplet state (T_1). Such isomerizations follow either an adiabatic or a diabatic mechanism.[11,12] In the first mechanism, the isomerization proceeds completely on the T_1 state potential energy surface (PES), and the product is formed in the excited state from which it decays to S_0. For olefins that isomerize according to a diabatic mechanism, decay to the ground state occurs at an intermediate perpendicularly twisted geometry (^{3}p*) that represents the minimum on the T_1 PES, and the products are formed on the S_0 surface. For a T_1 state *Z*/*E*-isomerization to proceed exclusively by the adiabatic mechanism, it has been concluded that the ^{3}p* structure must be at least 7 kcal/mol higher in energy than the planar T_1 structure of the olefin.[12] The adiabatic mechanism should be advantageous in technical applications of *Z*/*E*-photoisomerizations as it allows for quantum chain processes, catalysis, and one-way isomerizations from *Z*- to *E*-isomers.[4,13] For S_1 state *Z*/*E*-photoisomerizations, Zanirato, Olivucci, and co-workers recently outlined the requirements for an efficient photoisomerization proceeding with a high quantum yield leading to olefins with optimal function as molecular switches.[14] It was concluded that the excited reactant (olefin) should travel along a barrierless pathway on the excited PES, decay to the ground state at a real surface crossing, and relax to the minimum corresponding to the photoproduct. For the T_1 state, we reason that an efficient isomerization pathway of an optically active molecular switch should involve a shallow barrier on the T_1 PES increasing the adiabatic isomerization mode and that decay to the ground state should occur from the excited product. It is also important that the pathway does not involve an intermediate on the T_1 PES. As a first step toward general principles that allow design of olefins with the desired T_1 state surface profiles, we explored the connection between the aromatic character of an olefin substituent and the shape of the T_1 PES for *Z*/*E*-isomerization of the olefin. In this regard, we particularly exploit Baird's theory on triplet-state aromaticity. At present, we focus on olefins with one monocyclic annulenyl substituent which allows for an unambiguous analysis of the effect of substituent aromaticity on the profile of the T_1 PES. The *Z*/*E*-photoisomerization of olefins with polycyclic substituents has more complex dependencies on the properties (T_1 energies and (anti)-aromaticities)) of the substituents.

Outline of Qualitative Theory. Earlier, we showed that the aromaticity of the phenyl group in styrene varies along the PES path describing the twist around the olefinic C=C bond in T_1 (cf. the T_1 state *Z*/*E*-isomerization of a substituted styrene).[15] Styrene should, according to Baird's theory, be partially antiaromatic in the planar T_1 structure (Scheme 1), and reaction pathways that reduce this character are favorable. In the ^{3}p* structure, the two 2p(C) orbitals of the olefinic bond are orthogonal, which allows for formation of a 1,2-biradical[16] and for regaining aromaticity for the phenyl group. This regaining of aromaticity is confirmed by calculated geometries and spin densities in T_1,[15] and it should be a leading factor in the existence of a minimum at ^{3}p* in styrene.[17]

Olefins with S_0 antiaromatic substituents (e.g., vinylcyclobutadiene; Scheme 1) should behave in a manner opposite that of olefins with S_0 aromatic substituents, as the former will be aromatic in their planar T_1 structures. Twist of the C=C bond to ^{3}p* should raise the energy since the T_1 aromatic character of the $4n\pi$-electron annulenyl substituent is disrupted when one of the radicals is forced to reside on C_β of the olefin (Scheme 1). As a result, the T_1 PESs of such olefins should have

(4) (a) Saltiel, J.; Sun, Y.-P. In *Photochromism: Molecules and Systems*; Durr, H., Bouas-Laurent H., Eds.; Elsevier: Amsterdam, 1990; p 64. (b) Görner, H.; Kuhr, H. J. *Adv. Photochem.* **1995**, *19*, 1.

(5) (a) Moniruzzaman, M.; Sabey, C. J.; Fernando, G. F. *Macromolecules* **2004**, *37*, 2572. (b) Aerts, G.; Wuyts, C.; Dermaut, W.; Geovaerts, E.; Geise, H. J.; Blockhuys, F. *Macromolecules* **2004**, *37*, 5406. (c) Frantz, R.; Durand, J.; Lanneau, G. F. *J. Organomet. Chem*. **2004**, *689*, 1867. (d) Zheng, P.; Hu, X.; Zhao, X.; Li, L.; Tam, K. C.; Gan, L. H. *Macromol. Rapid Commun*. **2004**, *25*, 678.

(6) *Molecular Switches*; Feringa, B. L., Ed.; Wiley-VCH: Weinheim, Germany, 2001.

(7) (a) Feringa, B. L.; Jager, W. F.; de Lange, B. *J. Am. Chem. Soc.* **1991**, *113*, 5468. (b) Feringa, B. L.; van Delden, R. A.; Koumura, N.; Geertsema, E. M. *Chem. Rev.* **2000**, *100*, 1789. (c) Koumura, N.; Geertsema, E. M.; van Gelder, M. B.; Meetsma, A.; Feringa, B. L. *J. Am. Chem. Soc.* **2002**, *124*, 5037. (d) ter Weil, M. K. J.; van Delden, R. A.; Meetsma, A.; Feringa, B. L. *J. Am. Chem. Soc.* **2003**, *125*, 15076. (e) van Delden, R. A.; Huck, N. P. M.; Piet, J. J.; Warman, J. M.; Meskers, S. C. J.; Dekkers, H. P. J. M.; Feringa, B. L. *J. Am. Chem. Soc.* **2003**, *125*, 15659. (f) ter Wiel, M. K. J.; van Delden, R. A.; Meetsma, A.; Feringa, B. L. *J. Am. Chem. Soc.* **2003**, *125*, 15076. (g) van Delden, R. A.; Koumura, N.; Schoevaars, A.; Meetsma, A.; Feringa, B. L. *Org. Biomol. Chem.* **2003**, *1*, 33. (h) van Delden, R. A.; van Gelder, M. B.; Huck, N. P. M.; Feringa, B. L. *Adv. Funct. Mater.* **2003**, *13*, 319. (i) van Delden, R. A.; Huck, N. P. M.; Piet, J. J.; Warman, J. M.; Meskers, S. C. J.; Dekkers, H. P. J. M.; Feringa, B. L. (j) van Delden, R. A.; Mecca, T.; Rosini, C.; Feringa, B. L. *Chem.*−*Eur. J.* **2004**, *10*, 61. (k) van Delden, R. A.; ter Wiel, M. K. J.; Feringa, B. L. *Chem. Commun.* **2004**, 200. (l) van Delden, R. A.; ter Wiel, M. K. J.; de Jong, H.; Meetsma, A.; Feringa, B. L. *Org. Biomol. Chem.* **2004**, *2*, 1531.

(8) Andreasson, J.; Kodis, G.; Terazono, Y.; Lidell, P. A.; Bandyopadhyay, S.; Mitchell, R. H.; Moore, T. A.; Moore, A. L.; Gust, D. *J. Am. Chem. Soc.* **2004**, *126*, 15926.

(9) Zhang, C.; Du, M.-H.; Cheng, H.-P.; Zhang, X.-G.; Roitberg, A. E.; Krause, J. L. *Phys. Rev. Lett.* **2004**, *92*, 158301.

(10) Jousselme, B.; Blanchard, P.; Gallego-Planas, N.; Levillain, E.; Delaunay, J.; Allain, M.; Richomme, P.; Roncali, J. *Chem.*−*Eur. J.* **2003**, *9*, 5297.

(11) (a) Arai, T.; Tokumaru, K. *Chem. Rev.* **1993**, *93*, 23. (b) Kanna, Y.; Arai, T.; Tokumaru, K. *Bull. Chem. Soc. Jpn.* **1993**, *66*, 1482.

(12) Arai, T. In *Organic Molecular Photochemistry*; Ramamurthy, V., Schanze, K. S., Eds.; Marcel Dekker: New York, 1999; p 131.

(13) (a) Sundahl, M.; Wennerström, O. *J. Photochem. Photobiol., A* **1996**, *98*, 117. (b) Brink, M.; Jonson, H.; Sundahl, M. *J. Photochem. Photobiol., A* **1998**, *112*, 149.

(14) Sampedro, D.; Migani, A.; Pepi, A.; Busi, E.; Basosi, R.; Latterini, L.; Elisei, F.; Fusi, S.; Ponticelli, F.; Zanirato, V.; Olivucci, M. *J. Am. Chem. Soc.* **2004**, *126*, 9349.

(15) Brink, M.; Möllerstedt, H.; Ottosson, C.-H. *J. Phys. Chem. A* **2001**, *105*, 4071.

(16) Caldwell, R. A.; Zhou, L. *J. Am. Chem. Soc.* **1994**, *116*, 2271.

(17) Ni, T.; Caldwell, R. A.; Melton, L. A. *J. Am. Chem. Soc.* **1989**, *111*, 457.

SCHEME 1

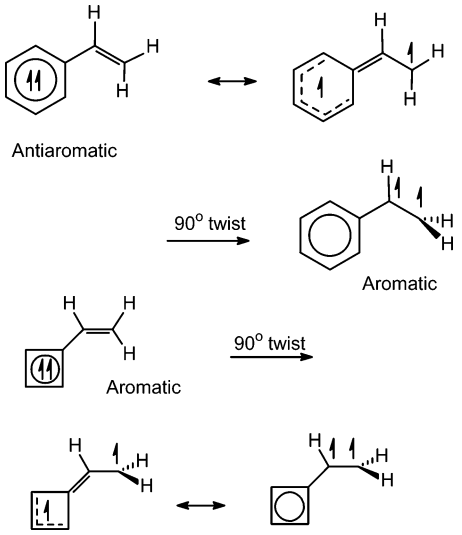

CHART 1

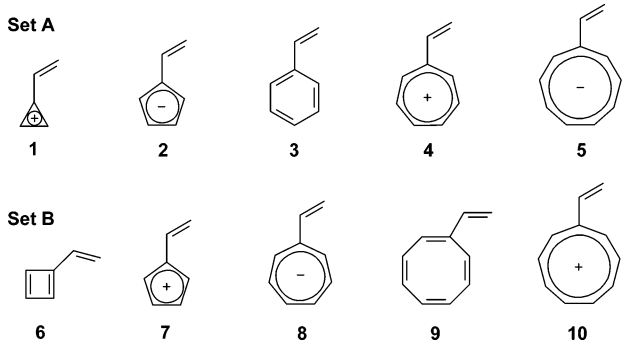

maxima at ^{3}p*. This relationship is supported by Hückel MO (HMO) theory since the Hückel energy of planar vinylcyclobutadiene in T_1 is $6\alpha + 6.602\beta$, whereas it is $6\alpha + 5.596\beta$ for the ^{3}p* structure calculated as one methyl radical and one methylenecyclobutadienyl radical. On the other hand, for planar styrene the Hückel energy in T_1 is $6\alpha + 9.100\beta$, whereas it is $6\alpha + 8.720\beta$ for the ^{3}p* structure calculated as one methyl radical and one benzyl radical. Even though the ^{3}p* structure of styrene is destabilized, this destabilization is much smaller than that for vinylcyclobutadiene (0.380β versus 1.006β), and this reflects the energetic behavior in T_1 of olefins with S_0 antiaromatic substituents versus those with S_0 aromatic substituents.

To validate our hypothesis on changes in aromaticity along the T_1 state *Z*/*E*-isomerization pathways of different olefins and to test its importance for the profile of the T_1 PESs, we compared various calculated properties of olefins with $(4n + 2)\pi$-electron substituents (**1**−**5**, set **A**; Chart 1) with those of olefins with $4n\pi$-electron substituents (**6**−**10**, set **B**). Even though **1**−**10** cannot *Z*/*E*-isomerize since C=C bond rotation leads to an equivalent structure, these compounds are models for more extensively substituted olefins. With strongly S_0 aromatic and strongly S_0 antiaromatic substituents the olefins in sets **A** and **B**, respectively, represent the two extremes between which the profiles of the T_1 PESs for olefinic C=C bond twist can vary. Even though well-suited for computations, set **B** olefins are less suited for experimental studies because of their generally very low stability and their small singlet−triplet energy gaps. For neither set did we consider annulenyl substituents with more than nine C atoms in the ring since differences in angle strain of planar and twisted structures influence too strongly their relative stabilities and bias the analysis. Hückel MO theory reveals that the results on the relative energies of the planar and perpendicularly twisted T_1 structures of styrene and vinylcyclobutadiene can be generalized to sets **A** and **B** olefins, respectively, as Figure 1 shows a zigzag relationship of the HMO energy differences on the numbers of π-electrons of the substituent. For the HMO energies of **1**−**10** in T_1, see the Supporting Information.

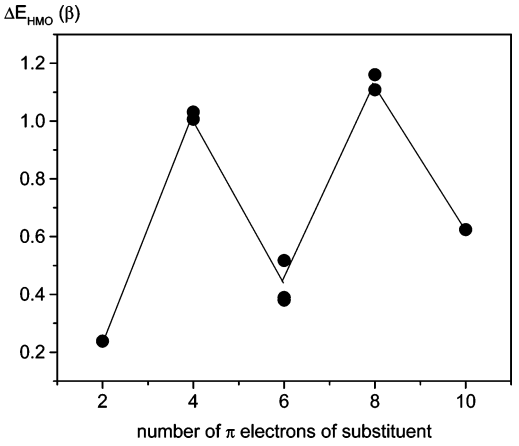

FIGURE 1. Differences in Hückel energies (ΔE_{HMO}) of **1**−**10** in their planar and perpendicularly twisted T_1 structures plotted against the number of π-electrons of the substituent.

Qualitative reasoning and HMO theory thus point to an interesting change in character of the T_1 PES, when going from olefins with $4n\pi$-electron substituents to those with $(4n + 2)\pi$-electron substituents. To obtain a quantitative measure of these changes, we performed more elaborate quantum chemical calculations of energies, spin densities, geometries, harmonic oscillator measure of aromaticity (HOMA),[18] and NICS[3] at planar olefin structures in S_0 and T_1, and at the perpendicularly twisted ^{3}p* structures in T_1. The calculated properties were used to assess the change in aromaticity upon excitation from S_0 to T_1 and along the T_1 reaction pathway that corresponds to the *Z*/*E*-isomerization pathway of more complex olefins. It is our belief that these results can provide guidance in the design of novel olefins that isomerize adiabatically in the T_1 state and, by extension, also in the S_1 state. We reason that increased knowledge about the fundamental properties that govern the profiles of excited-state PESs of olefins that *Z*/*E*-isomerize will be helpful to design improved optical switches and memories that display high photoisomerization quantum yields.

Computational Methods

The computations were done with the Gaussian03 and Molcas version 6 program packages.[19,20] Geometries were

(18) Krygowski, T. M. *J. Chem. Inf. Comput. Sci*. **1993**, *33*, 70.
(19) Frisch, M. J., et al. *Gaussian 03*, revision B.05; Gaussian, Inc.: Pittsburgh, PA, 2001. See the Supporting Information for complete citation.
(20) Karlström, G.; Lindh, R.; Malmquist, P.-Å.; Roos, B. O.; Ryde, U.; Veryazov, V.; Widmark, P.-O.; Cossi, M.; Schimmelpfennig, B.; Neogrady, P.; Seijo, L. *Comput. Mater. Sci.* **2003**, *28*, 222.

optimized at the (U)OLYP density functional theory level, first using the 6-31G(d) basis set of Pople and Hariharan,[21] and thereafter the TZ2P basis set of Dunning.[22] Frequencies were calculated at the (U)OLYP/6-31G(d) level to verify that the stationary points correspond to minima or to the transition state for C=C bond twist. The OLYP method combines the OPTX exchange functional, developed by Handy and Cohen,[23] with the correlation functional of Lee, Yang, and Parr (LYP).[24] This DFT method gave better descriptions of olefins and radical compounds when compared to the corresponding BLYP values.[25] It also gave excellent agreement of lowest singlet−triplet state and lowest singlet−quintet state energy differences of fulvenes and fulvalenes when compared to CASPT2 results.[26] For **1**, **6**, and **7**, calculations were also carried out at the CASSCF and CASPT2 levels using the [C/4s3p2d, H/3s1p] atomic natural orbital (ANO) basis set.[27] The active space in these calculations comprise all the π-orbitals and intercalated σ-orbitals, resulting in 10 active orbitals for **1** and 12 active orbitals for **6** and **7**. The active space contained 10 electrons for **1** and 12 electrons for **6** and **7**.

Mulliken spin densities were calculated at the (U)OLYP/TZ2P level, and the $\langle S^2 \rangle$ values never exceeded 2.02 in any calculations (i.e., close to the ideal value of 2.0). Subsequently, NICS values, as magnetic estimates of aromaticity, were calculated at the GIAO-OLYP/TZ2P+//OLYP/TZ2P[28] level of theory. The exponent of the diffuse function ($\alpha_{diffuse}$) was calculated according to the method of Lee and Schaefer.[29] It should be noted that NICS values are preferably calculated at a distance of 1.0 Å outside the ring planes (NICS(1)), due to the strong local shielding effects of the σ_{CC} and σ_{CH} bonds that dominate NICS values calculated at ring centers.[30] However, herein we discuss NICS calculated at the ring center (NICS(0)), because of the difficulty to apply NICS(1) to distorted ring structures due to the ambiguity in selection of the ring plane.

Geometry is also an important indicator of aromaticity. A universal and quantitative geometric measure of aromaticity is HOMA,[18] defined as

$$\mathrm{HOMA} = 1 - \frac{\alpha}{n}\sum(R_{opt} - R_i)^2 \qquad (1)$$

where n is the number of bonds and α is the normalization constant (257.7 for CC bonds). For an ideal aromatic system HOMA = 1 as such a system has all bonds equal to the optimal value R_{opt} (1.388 Å for CC bonds). The R_i is the bond length of each individual CC bond. With these parameters the HOMA value of benzene is 0.969 when based on the geometry from electron diffraction measurements.[18] However, R_{opt} and α were derived for the singlet ground state, and it is not likely that the same values are optimal for T_1 because a triplet state aromatic system (e.g., cyclooctatetraene, COT) has longer C−C bonds in T_1 than benzene in S_0 (r_{CC} = 1.408 Å in T_1 state cyclooctatetraene and 1.397 Å in S_0 state benzene at the OLYP/TZ2P level). Some caution will therefore be exercised when analyzing the HOMA values of the T_1 states.

Results and Discussion

The results will be presented and discussed in the following order: relative energies, spin densities, geometries (bond lengths and HOMA values), and finally NICS values. Thus, we first probe the stabilization/destabilization upon twist around the C=C bond and subsequently assess the changes in aromaticity by geometric and magnetic measures. If otherwise not noted, the energies, geometries, HOMA values, and spin densities stem from (U)OLYP/TZ2P calculations.

Energies. There is a vast difference in the triplet state energies (E_T) between the olefins of set **A** and those of set **B**. The planar olefin structures in set **A** have E_T in the range 51.4−69.5 kcal/mol, whereas those in set **B** have E_T in the range 1.3−20.6 kcal/mol. For the vinylcyclopentadienyl cation **7**, the lowest triplet state is of similar energy as the lowest singlet state because it is found at 1.3 and −1.7 kcal/mol relative to the singlet state at the (U)OLYP/TZ2P and CASPT2/[4s3p2d/3s1p]//OLYP/TZ2P levels, respectively. Indeed, Saunders et al. showed by EPR measurements that the cyclopentadienyl cation has a triplet ground state,[31] similar to that found for **7** at the CASPT2 level. This minute and reversed singlet−triplet energy splitting is explained by the theory of disjoint and nondisjoint biradicals of Borden and Davidson.[32] Only for disjoint biradicals for which the two half-filled nonbonded molecular orbitals (NBMOs) can be confined to two different sets of C atoms is the open-shell singlet state below the triplet state. However, for the cyclopentadienyl cation, the two NBMOs cannot be confined to two sets of C atoms and the triplet state is lowest. The (U)OLYP/TZ2P level also orders the two states of the cyclopentadienyl cation correctly with the triplet below the singlet state by 9.6 kcal/mol, similar to the CASPT2(14,15)/[4s3p2d/3s1p]//OLYP/TZ2P energy of 14.3 kcal/mol.[33]

In contrast, the planar biradical **6** can be dissected in two allyl radicals, and it can be deduced that the two NBMOs are confined to two sets of C atoms.[32] Therefore, **6** has a singlet ground state, as does cyclobutadiene, and due to Jahn−Teller distortion of the cyclobutadiene ring their open-shell singlet states collapse to closed-shell singlets. For **6**, the E_T values calculated with (U)OLYP/TZ2P and CASPT2/[4s3p2d/3s1p]//OLYP/TZ2P are 5.2 and 6.0 kcal/mol. It can be seen that OLYP when evaluated against CASPT2 describes well the relative T_1 energies of **6** and **7**.

Upon twisting of the olefinic C=C bond to ^{3}p* structures, 1.2−10.6 kcal/mol are gained in set **A** at the OLYP/

(21) Hariharan, P. S.; Pople, J. A. *Theor. Chim. Acta* **1973**, *28*, 213.
(22) Dunning, T. H. *J. Chem. Phys.* **1971**, *55*, 716.
(23) Handy, N. C.; Cohen, A. J. *Mol. Phys*. **2001**, *99*, 403.
(24) Lee, C.; Yang, W.; Parr, R. G. *Phys. Rev. B* **1988**, *37*, 785.
(25) Baker, J.; Pulay, P. *J. Chem. Phys*. **2002**, *117*, 1441.
(26) Möllerstedt, H.; Piqueras, M. C.; Crespo, R.; Ottosson, H. *J. Am. Chem. Soc.* **2004**, *126*, 13938.
(27) Widmark, P. O.; Persson, B. J.; Roos, B. O. *Theor. Chim. Acta* **1991**, *79*, 419.
(28) Wolinski, K.; Hilton, J. F.; Pulay, P. *J. Am. Chem. Soc.* **1990**, *112*, 8251.
(29) Lee, T. J.; Schaefer, H. F. *J. Chem. Phys*. **1985**, *83*, 1784.
(30) (a) Schleyer, P. v. R.; Jiao, H.; Hommes, N. J. R. v. E.; Malkin, V. G.; Malkina, O. L. *J. Am. Chem. Soc.* **1997**, *119*, 12669. (b) West, R. Y.; Buffy, J. J.; Haaf, M.; Müller, T.; Gehrhus, B.; Lappert, M. F.; Apeloig, Y. *J. Am. Chem. Soc.* **1998**, *120*, 1639.
(31) Saunders, M.; Berger, R.; Jaffe, A.; McBride, J. M.; O'Neill, J.; Breslow, R.; Hoffman, J. M., Jr.; Perchonock, C.; Wasserman, E.; Hutton, J. M.; Kuck, V. J. *J. Am. Chem. Soc.* **1973**, *95*, 3017.
(32) Borden, W. T.; Davidson, E. R. *J. Am. Chem. Soc.* **1977**, *99*, 4587.
(33) In addition to displaying a Jahn−Teller distortion reducing the symmetry of *c*-$C_5H_5^+$ from D_{5h} to C_{2v}, two singlet states with distinctly different geometries compete at being the lowest, as also observed earlier. See: (a) Borden, W. T.; Davidson, E. R. *J. Am. Chem. Soc.* **1979**, *101*, 3771. (b) Lee, E. P. F.; Wright, T. G. *Phys. Chem. Chem. Phys.* **1999**, *1*, 219. (c) Zilberg, S.; Haas, Y. *J. Am. Chem. Soc.* **2002**, *124*, 10683. The first state with the dominant configuration [...$(b_1)^2$-$(a_2)^2$] is lower than the second state with the dominant configuration [...$(b_1)^2(b_1)^2$] by 0.8 kcal/mol at the OLYP/TZ2P level and 0.5 kcal/mol at the CASPT2 level when using an active space of 12 electrons in 14 orbitals. However, the increase of the active space to 14 electrons in 15 orbitals in the CASPT2 calculation makes the second state more stable by 1.5 kcal/mol.

TABLE 1. Relative Energies of T_1 Structures of 1−10[a]

olefin		E(planar S_0) − E(T_1)	E(^{3}p*) − E(planar T_1)
1	planar T_1	69.5, *71.3* (*71.0*)	
	^{3}p*	58.9, *60.2* (*60.5*)	−10.6, *−11.2* (*−10.5*)
2	planar T_1	58.5	
	^{3}p*	58.0	−0.5
3	planar T_1	61.3	
	^{3}p*	55.6	−5.7
4	planar T_1	51.4	
	^{3}p*	50.3	−1.2
5	planar T_1	56.4	
	^{3}p*	46.6	9.8
6	planar T_1	5.2, *6.0* (*6.1*)	
	^{3}p*	26.8, *25.7* (*30.3*)	21.6, *19.7* (*24.3*)
7	planar T_1	1.3, *−1.7* (*−1.6*)	
	^{3}p*	28.1, *26.9* (*27.0*)	26.8, *28.6* (*28.5*)
8	planar T_1	3.1	
	^{3}p*	35.4	32.3
9	planar T_1	11.9	
	^{3}p*	40.2	28.4
10	planar T_1	20.6	
	^{3}p*	46.2	25.6

[a] Energies in kcal/mol. Values in normal print at the (U)OLYP/TZ2P level, in italic at the CASPT2/[4s3p2d/3s1p]//(U)OLYP/TZ2P level, and in parentheses italic at the CASPT2/[4s3p2d/3s1p]//CASSCF/[4s3p2d/3s1p] level.

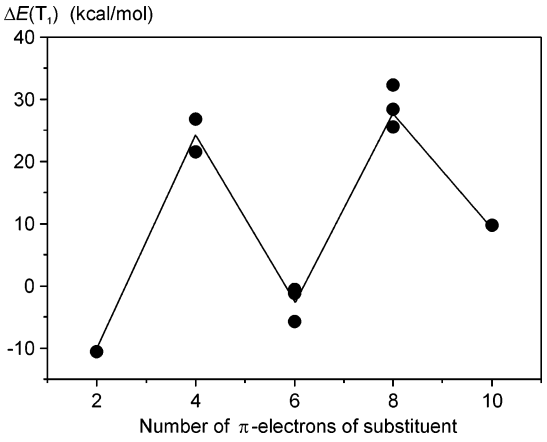

FIGURE 2. Dependence of $\Delta E(T_1) = E(^3p^*) - E(\text{planar } T_1)$ on the number of π-electrons of the olefin substituent of **1**−**10**. Energies in kcal/mol from (U)OLYP/TZ2P calculations. Line points correspond to average values.

TZ2P level, but 21.6−32.3 kcal/mol are required in set **B** (Table 1). The CASPT2 energy differences between planar and perpendicularly twisted structures of **1**, **6**, and **7** are similar. Thus, the planar T_1 structures in set **A** are transition states along the pathway between two equivalent ^{3}p* structures, whereas for set **B** olefins the twisted structures represent transition states connecting two minima at equivalent planar T_1 structures of the olefin. As a result, the profile of the T_1 PES for twist around the olefinic C=C bond depends in a zigzag manner on the number of π-electrons of the olefin substituent (Figure 2), as suggested already by HMO theory (Figure 1). The stabilization of set **A** olefins and destabilization of set **B** olefins upon twist from the planar to the perpendicularly twisted T_1 structure is also in line with our hypothesis, which assumes that aromaticity is regained in the first set and lost in the second.

Disregarding the instability and minute E_T of **6**, this molecule represents, if two different substituents were to be attached at C_β, the smallest neutral annulenyl substituted olefin with a T_1 PES that in theory allows for an adiabatic *Z*/*E*-photoisomerization. Higher E_T values, leading to increased stability, are found in **9** and **10** since their 8π-electron substituents adopt puckered nonaromatic structures in S_0. However, the T_1 barriers for C=C bond twist among all set **B** olefins (21.6−32.3 kcal/mol) are too high for this process to occur at ambient temperatures because Arai and Takahashi found that a barrier higher than 15 kcal/mol gives very low T_1 state *Z*/*E*-photoisomerization quantum yields at room temperature.[34] Fortunately, olefins with less antiaromatic substituents than those in set **B** are more stable and should isomerize over barriers that are below 15 kcal/mol. Fusion of S_0 antiaromatic annulenyl rings with S_0 aromatic rings could also be a way to design substituents that yield olefins with more suitable T_1 PESs for adiabatic isomerizations.[35] Finally, a stabilization of the ^{3}p* structures of set **B** olefins through delocalization of the radical at C_β could be attained by attachment of a radical stabilizing group at this position.

TABLE 2. Calculated Spin Density Distribution of 1−10[a]

	planar T_1		^{3}p*	
olefin	aryl ring	olefin bond[b]	aryl ring	olefin bond[b]
1	0.46	1.54 (0.62 + 0.92)	0.30	1.70 (0.64 + 1.06)
2	0.88	1.12 (0.24 + 0.88)	0.40	1.60 (0.46 + 1.14)
3	0.90	1.10 (0.19 + 0.91)	0.31	1.69 (0.62 + 1.07)
4	1.02	0.98 (0.20 + 0.78)	0.46	1.54 (0.47 + 1.07)
5	1.68	0.32 (−0.13 + 0.45)	0.41	1.59 (0.47 + 1.12)
6	1.71	0.29 (−0.22 + 0.51)	0.99	1.01 (−0.13 + 1.14)
7	1.65	0.35 (−0.09 + 0.44)	1.06	0.94 (−0.20 + 1.14)
8	1.75	0.25 (−0.09 + 0.34)	1.06	0.94 (−0.25 + 1.19)
9	1.86	0.14 (−0.14 + 0.28)	1.03	0.99 (−0.16 + 1.15)
10	1.78	0.22 (−0.09 + 0.31)	0.77	1.23 (−0.17 + 1.40)

[a] Values in electron from UOLYP/TZ2P calculations [b] Mulliken spin density at C_α and C_β given in parentheses.

With the present theory we can now explain the inefficient isomerization of 1,5-bis(styryl)-3,7-dimethylcyclooctatetraene as due to the aromatic character of the COT ring in the T_1 state (*Z*/*E*-photoisomerization quantum yields of $\phi_{ZZ-EZ} = 0.0075$ and $\phi_{EZ-EE} = 0.0040$).[36] The localization of the triplet excitation to the COT ring leads to high barriers for twist around the two C=C bonds. The adiabatic mechanism was previously considered as the most likely mechanism, and the present calculations support this view. The low isomerization quantum yields at ambient temperatures are explained by a high T_1 barrier, similar to that found for perylenylethylene by Arai and Takahashi.[34]

The calculated energy profiles of sets **A** and **B** olefins, respectively, are thus in line with our hypothesis put forward in the Introduction. However, can these changes be related to an increase/decrease in T_1 aromaticity as one twists around the C=C bond?

Spin Densities. Calculated spin densities are shown in Table 2 and indicate the importance of various resonance structures. For set **B**, a large part of the triplet biradical character in planar structures is located in the

(34) Arai, T.; Takahashi, O. *J. Chem. Soc., Chem. Commun.* **1995**, 1837.
(35) Kato, H.; Akasaka, R.; Muthas, D.; Karatsu, T.; Ottosson, H. Manuscript in preparation.
(36) Anger, I.; Sundahl, M.; Wennerström, O.; Auchter-Krummel, P.; Müllen, K. *J. Phys. Chem.* **1995**, *99*, 650.

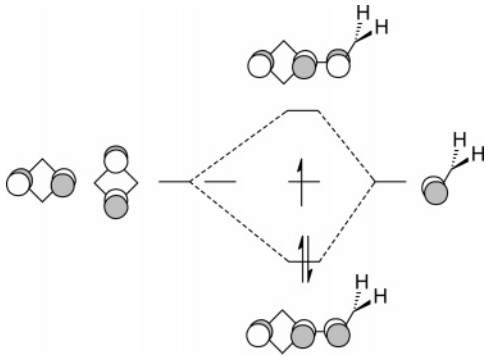

FIGURE 3. Interactions between isoenergetic A′ symmetric fragment orbitals in the methylenecyclobutadiene part of the ^{3}p* structure of **6**.

rings (total α-spin density (P_α) of ring C atoms is 1.65−1.86 e). Simultaneously, spin densities at the olefinic C=C bonds are low ($0.14 \le P_\alpha \le 0.35$ e), supporting the view that set **B** olefins have T_1 state aromatic substituents. In contrast, the ring substituents of the planar T_1 olefins **1**−**4** of set **A** have lower spin densities ($0.46 \le P_\alpha \le 1.02$ e), although the spin density is still high for **5** (1.68 e) because its cyclononatetraenyl ring is strongly puckered and can accommodate both radicals. Simultaneously, the C_β of the vinyl group of **1**−**4** has a high radical character ($0.78 \le P_\alpha \le 0.92$ e), whereas it is lower for **5** (0.45 e). In contrast, the spin density of C_α is much lower ($-0.13 \le P_\alpha \le 0.24$ e), except for **1** where it is 0.62 e. One of the two radicals is therefore essentially delocalized into the ring. For instance, in **3** this unpaired electron is delocalized to the two C_{ortho} ($P_\alpha = 0.21$ and 0.35 e, respectively) and C_{para} ($P_\alpha = 0.50$ e) atoms of the phenyl group. The situation is somewhat different for **1** with its planar structure because both unpaired electrons are pushed out from the ring to the vinyl group so that the cationic cyclopropenyl ring gains aromaticity. However, in general, the most important triplet biradical resonance structures of set **A** olefins have one unpaired electron at C_β and the other in the annulenyl ring. The T_1 antiaromaticity of the $(4n + 2)\pi$-electron annulene rings is thereby reduced through localization of one unpaired electron to the vinyl group.

In ^{3}p* structures, one of the unpaired α-electrons is forced to reside on C_β, and the two unpaired electrons can reside in two orthogonal AOs. Because aromaticity was regained, this implies that the perpendicularly twisted T_1 structures of set **A** olefins tend toward 1,2-biradicals (P_α (C_α) = 0.46−0.64 e and P_α (C_β) = 1.06−1.14 e, respectively). On the other hand, twist of the C=C bond in set **B** olefins forces the T_1 aromaticity of the annulenyl rings to be disrupted. The ^{3}p* structures of set **B** olefins are also not 1,2-biradicals since the C_α atom spin densities range only from −0.25 to −0.13 e. Qualitatively, this finding can be understood for ^{3}p*-**6** by considering the isoenergetic orbital interaction in the methylenecyclobutadienyl radical of ^{3}p*-**6** between the localized NBMOs of cyclobutadiene and the 2pπ AO of the methylene fragments (Figure 3). This radical can be viewed as an allyl radical since one of the three electrons of the A′ symmetric MOs occupies the NBMO of cyclobutadiene which does not interact with the 2pπ AO of the methylene fragment. This qualitative MO picture of ^{3}p*-**6** is supported by calculations since C4 and C6 of the cyclobutadienyl ring have the largest spin densities (0.70 and 0.72 e, respectively).

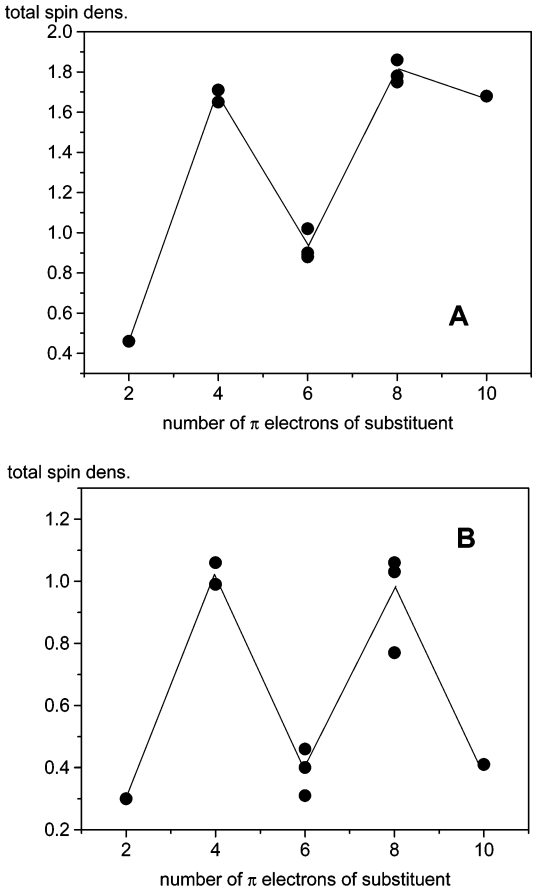

FIGURE 4. Calculated spin densities of aryl rings at the UOLYP/TZ2P level of (A) planar T_1 structures and (B) perpendicularly twisted T_1 structures.

If the amount of spin density in the ring substituents at, respectively, planar and perpendicularly twisted T_1 structures is plotted against the number of π-electrons of the substituents, then a zigzag relationship can be noted (Figure 4), similar to the energy. At planar T_1 structures the rings of set **B** olefins host nearly two unpaired electrons indicating T_1 aromaticity according to Baird, whereas at perpendicularly twisted T_1 structures the rings of set **A** olefins have low spin densities in the range 0.30−0.46 e indicating that these rings tend toward closed-shell S_0 aromaticity at these structures. We note that **5** in its planar T_1 structure of the olefin bond can pucker the cyclononatetraenyl group and host both radicals leading to its high spin density value in Figure 4A.

To quantify the aromaticity of an annulenyl ring, energetic, geometric, and magnetic measures can be applied. We make use of geometric and magnetic measures because an unambiguous energetic measure is difficult to realize for our systems. Lately, there has been some debate as to whether linear correlations should exist between the various measures of aromaticity.[37] Moreover, aromaticity is defined as a ground-state property, and if applied to the triplet excited state its multidimensional character becomes even more pro-

nounced.[38] However, we now argue that when different aromaticity probes all display similar zigzag variations in their values upon going from planar to perpendicularly twisted T_1 structures on the number of π-electrons of the substituent, then the variation in aromaticity along the T_1 PES of substituted olefins should be verified.

Geometries. For adiabatically *Z*/*E*-photoisomerizing annulenyl olefins, the T_1 excitation should be localized to the annulenyl group, whereas for those that isomerize diabatically it is localized to various extents to the C=C bond.[39] These excitation localizations are reflected in the geometry changes of **1**−**10** that take place upon excitation from S_0 to T_1. The vinylic C=C bond elongations of 0.087−0.110 Å in set **A** indicate olefin excitations (Figure 5), whereas the corresponding bond elongations of merely −0.007 to 0.019 Å in set **B** reveal ring excited T_1 states (Figure 6). Interestingly, the vinylic C=C bond in **8** is even shortened slightly upon excitation. A successively reduced localization of the excitation to the olefin will naturally lead to a gradually higher rotational barrier for the *Z*/*E*-photoisomerization.[8]

The CC bond lengths of the annulenyl groups reveal how the aromaticity in T_1 differs for sets **A** and **B** olefins and how it changes along the T_1 isomerization pathway. Upon excitation to the planar T_1 structures, the variation in these bond lengths (Δr_{CC}(Ar) = longest r_{CC} − shortest r_{CC} of the ring) increases for set **A** olefins (0.017−0.037 Å in S_0 versus 0.041−0.106 Å in T_1) but decreases for set **B** olefins (0.125−0.242 Å in S_0 versus 0.031−0.085 Å in T_1). This behavior supports Baird's theory on reversal of aromaticity and antiaromaticity when going from S_0 to T_1.[1]

The cyclooctatetraenyl ring in **9** also adopts a planar structure in T_1, contrary to the situation in S_0. This is in line with the D_{8h} symmetric structure of T_1 cyclooctatetraene previously found by Gogonea et al.,[2] which indicates that the stabilization by aromaticity is larger than the increase in angle strain. The ring in **10** is slightly puckered in T_1 but much less than in S_0, also in line with previous calculations.[2] As noted above, the cyclononatetraenyl group in the planar T_1 structure of **5** is puckered, but upon twist it tends toward planar again, in accordance with some antiaromatic character at the planar T_1 olefin structure, but regains aromaticity at the ^{3}p* structure.

Loss of aromaticity when going from planar to twisted T_1 structures of set **B** olefins, and regaining aromaticity when going to these structures of set **A** olefins, also shows up in the CC bonds lengths of the annulenyl groups. The $\Delta\Delta r_{CC}$(Ar, T_1) = Δr_{CC}(Ar, planar T_1 structure) − Δr_{CC}(Ar, twisted T_1 structure) takes negative values between −0.061 and −0.017 Å in set **A** olefins, but adopts positive values ranging from 0.011 to 0.054 Å in set **B** olefins. Thus, a zigzag dependence is once again obtained (Figure 7), now between the number of π-electrons of the substituent and $\Delta\Delta r_{CC}$(Ar, T_1). This reveals that changes in aromaticity and antiaromaticity, which depend on the nature of the olefin substituent, take place along the T_1 energy surface. Interestingly, the shortenings in $\Delta\Delta r_{CC}$(Ar, T_1) upon twist of set **A** olefins are similar to the lengthenings in set **B** olefins.

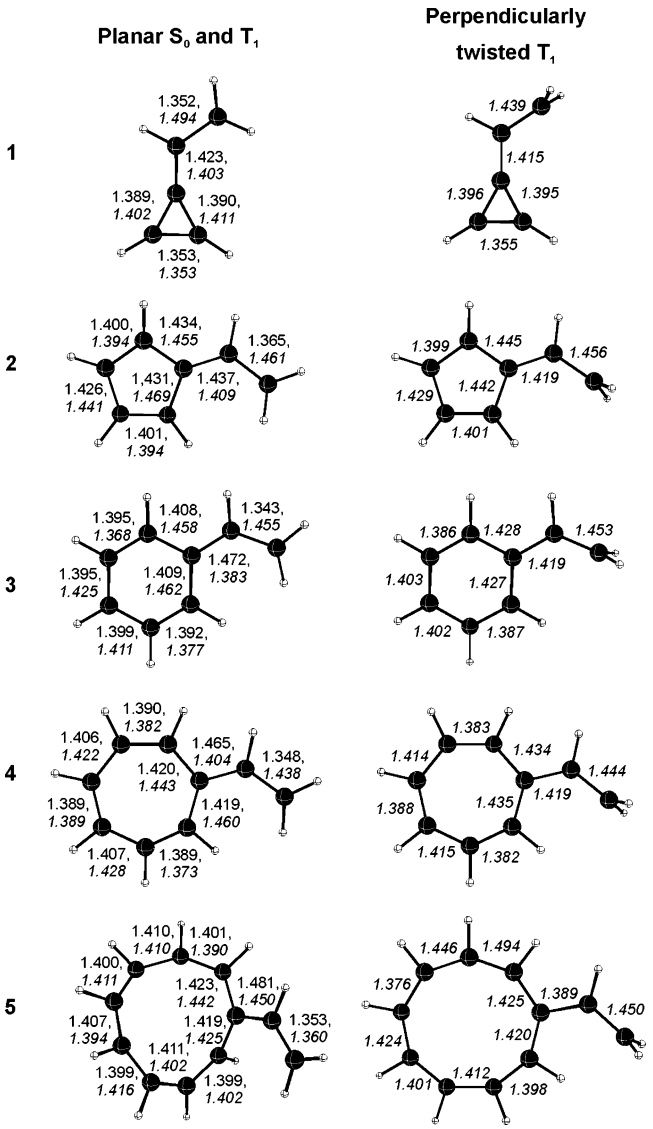

FIGURE 5. Calculated geometries of set **A** olefins **1**−**5** at planar S_0, planar T_1, and perpendicularly twisted T_1 structures at the (U)OLYP/TZ2P level. The T_1 structures are displayed. Bond lengths in Å for the S_0 state are in normal print, and bond lengths for the T_1 state are in italics.

A quantitative geometric measure of the aromaticity changes that occur upon excitation from S_0 to T_1 and along the T_1 PES is provided by the HOMA values (Table 3). Figure 8 shows the dependence of ΔHOMA(T_1) = HOMA(^{3}p*) − HOMA(planar T_1) on the number of π-electrons of the olefin substituent of **1**−**10**. However, some caution should be exercised because the HOMA parameters were derived for the singlet ground state, and they will likely not be optimal for triplet state aromatic compounds. In S_0, the HOMA values of set **A** olefins are in the range from 0.705 to 0.954, indicating aromaticity, and they are reduced in both planar and perpendicular olefin structures in T_1, except for **1**. This latter finding is also obtained when basing the HOMA calculations on

(37) (a) Katritzky, A. R.; Karelson, M.; Sild, S.; Krygowski, T. M.; Jug, K. *J. Org. Chem.* **1998**, *63*, 5228. (b) Sakai, S. *J. Phys. Chem. A* **2002**, *106*, 10370. (c) Poater, J.; Fradera, X.; Duran, M.; Solà, M. *Chem.−Eur. J.* **2003**, *9*, 400.

(38) Schleyer, P. V. R.; Jiao, H. *Pure Appl. Chem.* **1996**, *68*, 209.

(39) (a) Kikuchi, O.; Segawa, K.; Takahashi, O.; Arai, T.; Tokumaru, K. *Bull. Chem. Soc. Jpn.* **1992**, *65*, 1463. (b) Segawa, K.; Takahashi, O.; Kikuchi, O.; Arai, T.; Tokumaru, K. *Bull. Chem. Soc. Jpn.* **1993**, *66*, 2754.

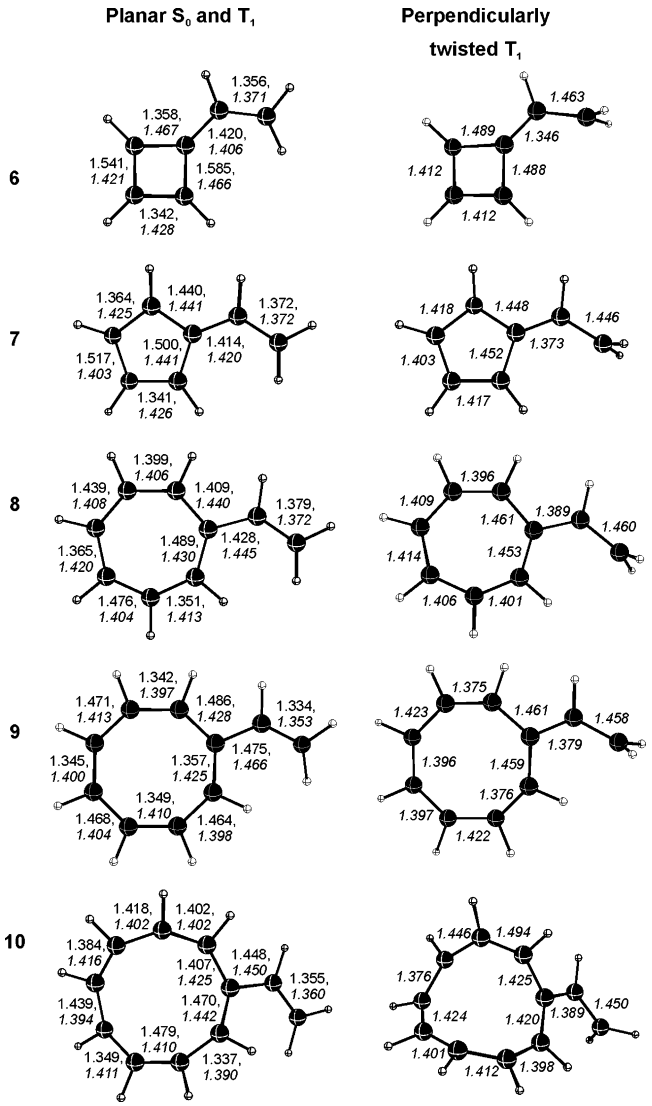

FIGURE 6. Calculated geometries of set **A** olefins **6**−**10** at planar S_0, planar T_1, and perpendicularly twisted T_1 structures at the (U)OLYP/TZ2P level. The T_1 structures are displayed. Bond lengths in Å for the S_0 state are in normal print, and bond lengths for the T_1 state are in italics.

the CASSCF geometries (Table 3). Planar set **A** olefin structures in T_1 adopt HOMA values lower than those of the perpendicular olefin structures, in line with our hypothesis on regaining aromaticity and formation of 1,2-biradical at the latter olefin structures. However, the opposite applies for set **B** olefins. Their HOMA values in S_0 are negative for **6** and **7**, indicating antiaromatic character, and close to zero for **8** and **9**, indicating nonaromatic character. Notably, the planar olefin structures in the T_1 state become aromatic, except for **6**, which becomes more nonaromatic. At perpendicular T_1 olefin structures the aromaticity of the substituents is reduced. The large difference in ΔHOMA(T_1) values calculated for **6** and **7** is found at both the OLYP and CASSCF levels (Table 3). Olefin **7** should, according to HOMA, reveal very small aromaticity changes when the C=C bond is twisted, and it also displays the smallest $\Delta\Delta r_{CC}$(Ar) and ΔP_α(Ar) among set **B** olefins.

Nucleus Independent Chemical Shifts. Changes in aromaticity upon excitation from S_0 to T_1 and along the

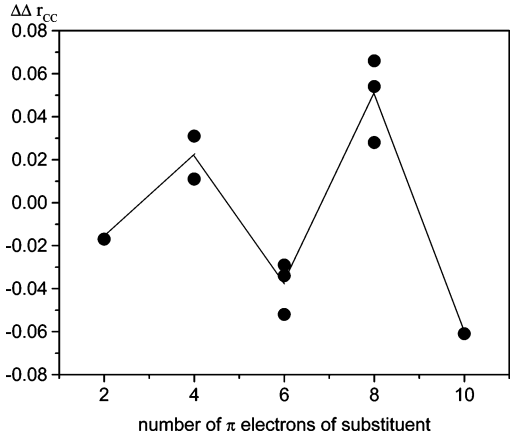

FIGURE 7. Dependence of $\Delta\Delta r_{CC}$(Ar; T_1) = Δr_{CC}(Ar; ^{3}p* structure) − Δr_{CC}(Ar; planar T_1 structure) on the number of π-electrons of the olefin substituent of **1**−**10**. Distances in Å from (U)OLYP/TZ2P calculations. Line points correspond to average values.

TABLE 3. Calculated HOMA Values of 1−10[a]

olefin	S_0	planar T_1	^{3}p*
1	0.894, *0.878*	0.832, *0.887*	0.897, *0.898*
2	0.705	0.281	0.581
3	0.954	0.450	0.848
4	0.901	0.587	0.787
5	0.882,	0.575	0.795
6	−3.177, *−3.291*	0.033, *−0.518*	−0.376, *−1.015*
7	−0.787, *−1.264*	0.554, *0.510*	0.502, *0.593*
8	0.153	0.740	0.587
9	−0.131	0.850	0.575
10	0.336	0.812	0.448

[a] Values in normal print at the OLYP/TZ2P level and values in italics at the CASSCF/[4s3d2p/3s1p] level.

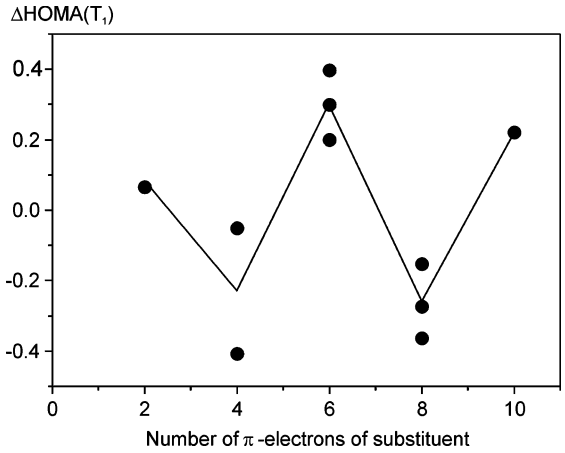

FIGURE 8. Dependence of ΔHOMA(T_1) = HOMA(^{3}p*) − HOMA(planar T_1) on the number of π-electrons of the olefin substituent of **1**−**10**. Results from (U)OLYP/TZ2P calculations. Line points correspond to average values.

T_1 PES can also be monitored by NICS (Table 4). These values reveal that in S_0 the substituents of set **A** olefins are more aromatic than those in planar T_1 structures, and the opposite applies to those of set **B**, in line with Baird's theory on interchange of aromaticity and antiaromaticity when going from S_0 to T_1.

The NICS(0) values also reveal that aromaticity is regained in the T_1 state upon twist of the vinylic C=C bonds in set **A** olefins, even though the annulenyl

TABLE 4. Nucleus Independent Chemical Shifts (NICS(0)) of 1−10 at the (U)OLYP/TZ2P+//(U)OLYP/TZ2P Level[a]

olefin	S_0	planar T_1	$^3p^*$
1	−22.2	−17.2	−20.1
2	−9.1	10.9	−6.4
3	−6.7	7.5	−3.6
4	−3.5	27.2	1.8
5	−11.7	−0.8	−7.3
6	22.0	1.1	8.1
7	44.3	1.0	52.7
8	7.0	−4.5	13.4
9	6.5	−8.1	8.6
10	1.0	−5.9	3.8

[a] Values in ppm.

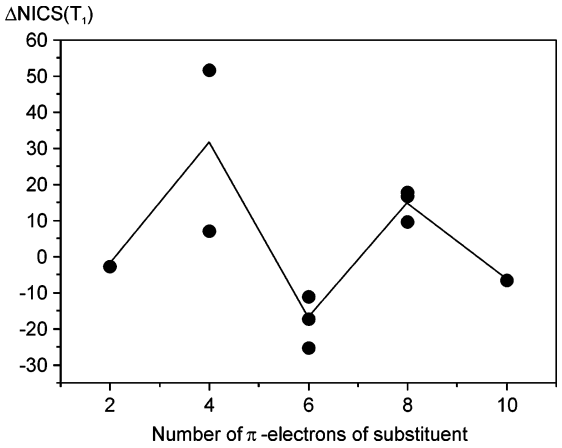

FIGURE 9. Dependence of $\Delta NICS(T_1) = NICS(^3p^*) - NICS(\text{planar } T_1)$ on the number of π-electrons of the olefin substituent of **1**−**10**. NICS values in ppm from GIAO-OLYP/TZ2P+//(U)OLYP/TZ2P calculations. Line points correspond to average values.

substituents do not become as aromatic in their $^3p^*$ structures as in their planar S_0 structures. The opposite applies to olefins in set **B** since their annulenyl groups become less aromatic when the vinylic C=C bond is twisted in T_1. Changes in substituent aromaticity on T_1 thus follow the profile of the T_1 PES; a decrease (increase) in aromaticity upon twist leads to a T_1 PES with a barrier (minimum) at $^3p^*$. Similar to the energy differences, spin densities, CC bond lengths of the annulenyl groups, and HOMA values, the differences in NICS(0) values between planar and perpendicularly twisted T_1 structures ($\Delta NICS(0)(T_1)$) also change in a zigzag manner when going successively from olefins with 2, 4, 6, 8, and 10 π-electron substituents.

As seen in Figure 9, **6** and **7** also display a large difference in $\Delta NICS(T_1)$, similarly to that found for the $\Delta HOMA(T_1)$ of these compounds. However, now **7** instead of **6** is the olefin that shows the large change upon twist of the C=C bond in T_1, thus revealing that geometric and magnetic measures of aromaticity do not always correlate, in line with earlier conclusions.[37] The large positive (antiaromatic) NICS values of **7** in S_0 are remarkable, but similar large values have been reported for the cyclopentadienyl cation (+54.8 ppm at the GIAO-HF/6-31G(d)//B3LYP/6-31G(d) level).[40] A value of 44.3 ppm is now calculated at the GIAO-OLYP/TZ2P+//OLYP/TZ2P level for this cation. The reduction of the NICS in **7** when compared to cyclopentadienyl cation should stem from weakening of the antiaromatic character by the vinyl group.

Thus, when comparing planar and perpendicularly twisted T_1 olefin structures all properties investigated herein vary more or less in a zigzag manner when successively increasing the number of π-electrons of the olefin substituent by two. This strong influence of the substituent on the T_1 state properties could likely be useful for tailoring olefins with targeted properties.

Summary and Outlook

Through quantum chemical calculations and application of Baird's theory on triplet state aromaticity, we demonstrate a strong relationship between the profile of the T_1 PES for twist around the C=C bond (cf. *Z*/*E*-isomerization) of an olefin with a monocyclic annulenyl substituent and the aromaticity and antiaromaticity of this substituent. For olefins with annulenyl substituents, the minimum on the T_1 PES corresponds to the olefin structure with highest substituent aromaticity. This implies that for olefins with monocyclic S_0 aromatic ($(4n + 2)\pi$-electron) substituents (set **A** olefins), such as styrene, the $^3p^*$ structures are the lowest point along the isomerization pathway, and for olefins with S_0 antiaromatic ($4n\pi$-electron) substituents (set **B** olefins), such as vinylcyclobutadiene, the planar T_1 structures are of lowest energy. The changes in energy of the T_1 state along the isomerization pathway, followed by changes in aromaticity, are reflected in CC bond lengths ($\Delta r_{CC}(Ar)$ and $\Delta HOMA$), as well as in magnetic measures ($\Delta NICS$) and spin densities. Zigzag relationships exist between the number of π-electrons of the monocyclic annulenyl substituents and these properties.

For olefins with polycyclic conjugated substituents, such as anthryl-substituted olefins, the dependence on aromaticity will be more complex since electron density will be shifted between the rings to maximize aromaticity in both S_0 and T_1 states. For example, in anthryl olefins in their planar T_1 structures, the triplet biradical character is localized largely to the central ring of the anthryl group, whereas the two outer rings remain S_0 aromatic. By twisting around the olefin C=C bond, one of the radicals is forced to reside at C_β of the olefin, presumably reducing the overall aromaticity of the anthryl group.

Since the profile of the T_1 PES, together with the spin−orbit coupling along the reaction coordinate, is a major factor that influences the fate of the olefin in the T_1 state, our finding on a connection between T_1 aromaticity change and T_1 PES profile should be valuable for design of novel substituted olefins that *Z*/*E*-isomerize adiabatically. Even though several of the systems investigated here are out of reach for experimental studies, the findings can be used to design novel olefins that isomerize adiabatically in T_1[35] and by extension also in the S_1 state. A better understanding of ways for influencing the profile of the excited-state surfaces of olefins should be helpful in the design of olefin-containing molecular switches and memories.

Acknowledgment. We are grateful to the Carl Trygger Foundation for financial support of a postdoc-

(40) Jiao, H.; Schleyer, P. v. R.; Mo, Y.; McAllister, M.; Tidwell, T. T. *J. Am. Chem. Soc.* **1997**, *119*, 7075.

toral fellowship to H.K. and to the Nationellt Superdatorcentrum (NSC) in Linköping, Sweden, for a generous allotment of computer time. M.C.P. and R.C. are grateful to the Generalitat Valenciana, MEC, and European Commission (IST-2001-32243) for financial support.

Supporting Information Available: Complete ref 19, Hückel energies, absolute energies, and Cartesian coordinates of compounds **1**−**10**. This material is available free of charge via the Internet at http://pubs.acs.org.

JO051558Y